Tailoring cream by modifying the composition of the fat and interfacial proteins to modulate stirred milk gel texture

Marine Moussier[a], Delphine Huc-Mathis[a], Camille Michon[a], Cyril Chaudemanche[b], Véronique Bosc[a,*]

a Ingénierie Procédés Aliments, AgroParisTech, Inra, Université Paris-Saclay, 91300 Massy, France

b Vienne Technical Centre, Yoplait/General Mills, Chemin des Mines, 38200 Vienne, France

*Corresponding author. Tel.: +33 169935120

E-mail address: veronique.bosc@agroparistech.fr (V. Bosc)

ABSTRACT

The formulation-structure-texture relationship in stirred emulsion-filled food gels has rarely been analysed, let alone in realistic conditions. By studying thermal (calorimetry), structural (laser diffraction, confocal microscopy and mathematical morphology analysis) and textural (rheology and tribology) properties, this work advanced the understanding of this relationship in stirred gels made entirely from milk ingredients. Indeed, tailoring the fat composition (AMF, olein or stearin fractions) and interfacial proteins (native or heat-aggregated WPI) in cream resulted in different properties. Crystallisation of the fat droplets and probably their interactions (aggregation or partial coalescence), pore size, microgel size and the coarseness of the protein network in stirred milk gels were all modified by the cream formulation. The changes in properties led to different textures and lubrication behaviours of the stirred milk gels. The highlighted relationships between formulation, structure and texture are recapitulated in a concluding diagram.

1. Introduction

Fatty dairy gels are complex systems in which fat is dispersed as droplets in a protein network. When stirred, this emulsion-filled gel becomes a concentrated dispersion of microgels between 10 and 100 µm in diameter (Lee & Lucey, 2010; Sodini, Remeuf, Haddad, & Corrieu, 2004). This type of food system is known for its sensory qualities and several authors reported that a reduction in fat content altered both flavour and textural properties, with reduced perception of the oily film, consistency, creaminess, thickness, creamy flavour or even firmness. Other authors demonstrated that reducing the fat content also reduced the storage modulus, apparent viscosity (at 100 s^{-1}), yield stress and lubrication properties (by increasing the friction coefficient) of different types of emulsion filled gel systems (Le Calvé et al., 2015; Liu, Stieger, van der Linden, & van de Velde, 2015; Lucey, Munro, & Singh, 1998; Sodini et al., 2004; Tomaschunas, Hinrichs, Köhn, & Busch-Stockfisch, 2012). Maintaining these properties is therefore essential if the fat content is to be reduced in such systems.

To be processed into stirred milk gel, milk undergoes typical unit operations involving different physico-chemical conditions, which modify the microstructure (Lee & Lucey, 2010; Sodini et al., 2004). Firstly, the milk is usually separated into skim milk and cream by centrifugation. Skim milk (about 3.5 wt% protein) is a colloidal suspension of casein micelles (30 to 600 nm in diameter (Cayot & Lorient, 1998)) also containing solubilised native whey proteins (WP) (about 5 nm in diameter), lactose and minerals. The cream is an oil-in-water emulsion (with about 35 wt% fat and 2 wt% proteins), in which the fat is dispersed as droplets about 5 µm in diameter, stabilised by a native membrane (Lopez, Briard-Bion, & Ménard, 2014). In standard dairy gel processing, the cream, the skim milk and sometimes skim milk powder (SMP) (with about 35 wt% protein) are mixed to obtain the target composition. The resulting mix is then pasteurised, homogenised (usually at 10 to 20 MPa) and gelled by acidification through fermentation.

Pasteurisation leads to the heat-induced aggregation of whey proteins and also to interactions between whey proteins and casein micelles via κ-casein (Donato & Guyomarc'h, 2009). As a result of homogenisation, the fat droplet size decreases to less than 1 µm and the native membrane is partially replaced (or newly formed) by WP and caseins (Cano-Ruiz & Richter, 1997). During acidification, the reduction in the pH from 6.5 to 4.5 reduces electrostatic repulsion between casein micelles and casein micelle/whey protein complexes, allowing them to interact and leading to the formation of a three-dimensional network. Micellar calcium (from calcium phosphate nanoclusters) is solubilised, thereby reducing interactions between caseins in the micelles. When applied, stirring breaks the continuous gel (i.e., set milk gel) into a concentrated dispersion of microgels about 10 µm in diameter (i.e., stirred milk gel) (Lee & Lucey, 2010; Sodini et al., 2004).

Many studies have demonstrated the impact of the interface and of fat composition on the texture of emulsion-filled gel systems. First, an increase in the solid fat content (SFC) was shown to increase the hardness of the droplets and hence the firmness of model emulsion-filled gels (Liu et al., 2015; Oliver, Scholten, & van Aken, 2015) and of set milk gels (Barrantes, Tamine, Sword, Muir, & Kalàb, 1996; Houzé, Cases, Colas, & Cayot, 2005). The fat droplets can also participate in the network via their interface, and the interaction between the proteins that form the gel network and the proteins adsorbed at the oil-in-water interface has been demonstrated in the case of model emulsion-filled gels (Sala, van Aken, Stuart, & van de Velde, 2007). In set milk gels, a threshold amount of 40% of the native membrane being replaced by milk proteins was shown to increase its storage modulus (G') (Michalski, Cariou, Michel, & Garnier, 2002). More specifically, Cho, Lucey, and Singh (1999) showed that the matrix was firmer (higher G') when whey protein concentrate (WPC) adsorbed at the interface was heat-aggregated than when it was native, which may be due to different interactive forces. In addition, some studies on emulsions showed that the interfacial composition impacted the crystallisation of fat in the droplets (Palanuwech & Coupland, 2003; Truong, Bansal, Sharma, Palmer, & Bhandari, 2014). Most of these studies were conducted either

on model systems or on set milk gels, whereas little is known about the combined effects of the interface and the fat compositions on the properties of stirred milk gels in realistic conditions.

The aim of this study was to understand the impact of the compositions of fat and interfacial proteins on the textural and structural properties of stirred milk gel systems, by designing tailored creams. On the one hand, the study was carried out under realistic formulation conditions, by using dairy ingredients and a process similar to that of stirred yoghurts. On the other hand, measurement conditions of stirred milk gels were chosen to take into account oral processing during the consumption of stirred yoghurts. The fat composition was controlled by using different fractionated milk fats and the interface by using either native or heat-aggregated whey protein isolate (WPI). First, the effect of the formulation on the thermal properties (fusion, solid fat content) and on the structural properties (fat droplet sizes) of the creams was evaluated. The impact of the different creams obtained on the textural properties (rheology, tribology), then structural properties (microgel sizes, protein network coarseness and pore size) of the resulting stirred milk gels were evaluated next. Finally, the relationship between formulation, structure and texture was analysed and is presented in a final diagram.

2. Materials and methods

2.1. Raw materials

Purified water was obtained using a Milli-Q purification system (Millipore, Merck, Germany), with a conductivity of 6.6×10^{-5} S m^{-1}. The skim milk powder (SMP) (18.4 wt% caseins, 6.7 wt% WP of which 68.1% was native) was provided by Eurosérum (Sodiaal, Port-sur-Saone, France). The whey protein isolate powder (WPI) (80.5 wt% WP of which 99.4% was native, 9.7 wt% caseins) was purchased from Lactalis (Laval, France) (95 wt% protein in dry matter) and glucono-δ-lactone (GDL) was purchased from Sigma-Aldrich (Saint-Quentin Fallavier, France). The pregelatinised modified rice starch was provided by Yoplait (Vienne, France) and the

anhydrous milk fat (AMF), its low melting temperature fraction (olein) and its high melting temperature fraction (stearin) were provided by Beuralia (Sodiaal, Quimper, France). The degree of unsaturation of the fats and their proportion of C18 fatty acids are listed in Table 1. Fatty acid composition was determined by gas chromatography coupled with mass spectrometry (GC-MS, Trace GC, Polaris Q, Thermo-Finnigan, Altricham, UK), with a ZB-WAX column (method adapted from NF EN ISO 12966-2).

2.2. Preparation of the creams

Solutions of WPI were prepared to reach a protein concentration of 1.2 wt% in the final creams. Each solution was prepared by dispersing WPI in Milli-Q water under continuous stirring for 15 min at room temperature and then kept overnight at 8 °C to ensure proper hydration. Some of the solutions were heat-treated under stirring at 80 °C for 30 min in a thermostatically controlled water bath. The resulting protein aggregates were approximately 100 nm in diameter (Dynamic light scattering, Nanosizer ZS, Malvern Instruments, UK, 1:100 dilution with Milli-Q water). Oil-in-water emulsions were prepared with either 60 wt% fat (for thermal analysis with DSC) or 30 wt% fat (for stirred milk gel production and all the other analyses). For this purpose, either the AMF, olein or stearin was melted at 60 °C for 30 min in a thermostatically controlled water bath before emulsification, and the corresponding WPI solution was tempered at 50 °C. After mixing the melted fat and the WPI solution, pre-homogenisation was performed with a rotor/stator (Polytron PT 3100 D, PTG 36/4 probe, Kinematica AG, Switzerland) at 15,000 rpm for 5 min. The resulting coarse emulsion was immediately treated by sonication (VCX 130, 13MM probe, Sonic & Materials, UK) at 130 W for 15 effective min (10 s pulses) to produce a fine emulsion. The temperature was maintained below the irreversible denaturation temperature of the whey proteins and the maximum temperature measured throughout the emulsification process never exceeded 55 ± 2 °C. All the information concerning the creams is listed in Table 2. In three different weeks, each

type of cream with 30 wt% fat was produced once, i.e., three repetitions of each. Creams with 60 wt% fat were made twice for thermal analysis.

2.3. Preparation of the stirred milk gels

Reconstituted skim milk was prepared by dispersing SMP in Milli-Q water under continuous stirring for 15 min at room temperature and then kept overnight at 8 °C to ensure proper hydration. Different milk mixes were prepared from the reconstituted skim milk and the different creams previously obtained, also adding 1 wt% of rice starch (as added in a reference recipe). The mixes were made to reach a target fat content of 6 or 10 wt%, and a target protein content of 3.1 wt%. Stirred milk gels were produced from each milk mix using the lab-scale process developed by Moussier, Huc-Mathis, Michon, & Bosc (2019b). The milk mixes were heat-treated in a thermostatically controlled water bath at 80 °C for 30 min under stirring and then sonicated (VCX 130, 13MM probe, Sonic & Materials, UK) at 130 W for 15 effective min (10 s pulses) to reproduce the homogenisation step. Once homogenised, they were cooled down to 30 °C and then acid-gelled for about 5 h (30 °C) by addition of 1 wt% GDL. After making sure the resulting gels had a pH below 4.55, they were stirred. The gels were first coarsely broken up with a spatula, poured into a beaker (1 L) and passed at 200 mL min^{-1} through two successive pipes (a first 40 cm long with a diameter of 7 mm, a second 100 cm long with a diameter of 3 mm) then through a filter (1 mm pores) using a peristaltic pump (L/S Precision Console, Masterflex, Gelsenkirchen, Germany).

In batches of 250 mL, the pre-stirred gels were ultra-smoothed by passing them once (from bottom to top) through a rotor/stator (Polytron PT 3100 D, PTG 36/4 probe, Kinematica AG, Switzerland) at 1,500 rpm. The stirred gels were finally placed in 100-mL pots at 26 ± 1.2 °C and stored at 8 °C for one week before being analysed. In three different weeks, each type of stirred milk gel was produced once, giving a total of three repetitions of each. All the information concerning the samples of stirred milk gel is listed in Table 2.

172

173 *2.4. Thermal analysis*

174

175 The thermal properties were analysed using differential scanning calorimetry (DSC) (DSC 1
176 STARe System, Mettler-Toledo, Greifensee, Swiss) and each measurement was systematically
177 made three times. Calibration was done using indium (initial melting temperature of 156.60 ± 0.30
178 °C, melting enthalpy variation of 28.45 ± 1.0 J g^{-1}). Approximately 20 mg of the pure bulk fat and
179 12 mg dry matter of the creams (60 wt% fat, 1.2 wt% proteins) were hermetically sealed in 40 µL
180 aluminum crucibles (Mettler-Toledo, Greifensee, Swiss). In the case of the creams, 0.8 M NaCl was
181 added to each to delay the crystallisation of water and hence improve the baseline. To avoid water
182 pressure during heating-cooling-heating kinetics, a hole was made in the crucibles using a needle.
183 Two types of heating-cooling-heating kinetics were performed to account for the conditions of
184 production and consumption of stirred milk gels as far as possible (Fig. 1). A temperature of 8 °C
185 was chosen as the standard temperature of household refrigerators, a cooling rate of 30 °C min^{-1} as
186 the average cooling rate throughout yoghurt production and a heating rate of 2 °C min^{-1} as a
187 compromise to be close to that of the mouth but also to be able to correctly measure melting
188 behaviour. Cooling down to 8 °C was followed by a quick quenching at –10 °C to obtain a good
189 baseline for the data treatment. The calorimetric parameters retrieved were those of melting. STARe
190 Excellence software (Mettler-Toledo, Greifensee, Swiss) was used to obtain the peak (T*peak*, °C)
191 and final (T*endset*, °C) melting temperatures as well the total variation in enthalpy (ΔH, J g^{-1}).
192 Based on the work of Lopez, Briard-Bion, Camier, & Gassi (2006), the order of magnitude of solid
193 fat content (SFC) formed by the emulsified AMF, olein and stearin fractions at 8 °C was calculated
194 using the following melting enthalpy ratio:

$$SFC\ (\%) = \frac{\Delta H_{partial}}{\Delta H_{total}} \qquad (1)$$

195 where ΔH*partial* (J g^{-1}) is the variation in the melting enthalpy of creams measured after cooling to
196 8 °C and ΔH*total* (J g^{-1}) is the one measured after cooling bulk fats down to –55 °C.

2.5. *Characterisation of the microstructure*

2.5.1. *Particle size distribution by laser diffraction*

The particle size distributions were obtained by laser diffraction with a MasterSizer 2000 (Malvern Instruments, UK). The size distributions of fat droplets were measured in the creams (Mie theory, 1.33 RI for water, 1.47 RI for milk fat) while the size distributions of the microgels were measured in the stirred milk gels (Fraunhofer theory). The creams (or stirred milk gels) were previously diluted 1:10 (w/w) with Milli-Q water. To achieve a constant level of obscuration (between 13 and 15%), only some drops of 1:10 diluted creams (or stirred milk gels) were poured in the dispersant tank for the measurement (three repetitions). The median diameters of fat droplets (or microgels) [d(0.5), µm] and the width of the distributions (span, eq. 2) were recovered.

$$span = \frac{d(0.9) - d(0.1)}{d(0.5)} \quad (2)$$

2.5.2. *Confocal laser scanning microscopy and quantitative analysis by mathematical morphology*

Confocal images were obtained with a TCS SP8 AOBS inversed confocal microscope (Leica, Solms, Germany) equipped with a helium-neon laser (458 nm excitation wavelength) and an argon laser (633 nm excitation wavelength). A two-step labeling protocol was implemented to stain fat and proteins, using the specific affinity properties of Bodipy 665/676 nm (Invitrogen, Carlsbad, NM, USA) and DyLight 488 nm (Thermo Fisher Scientific, Waltham, MA, USA), respectively. For each measurement, the fat image (in red) was superimposed on the protein image (in green). The images shown in this article were chosen as representative of the five replicates performed for each stirred milk gel. The replicates were obtained all at once for each type of stirred milk gel.

Quantitative analysis of the microstructure was possible from the protein confocal images using mathematical morphology, based on pixel transformations by dilations and erosions of an element with a side length of (2n+1) pixels (element side of 3 pixels with n = 1, 40 erosions, 40 dilatations) (Fenoul, Le Denmat, Hamdi, Cuvelier, & Michon, 2008). In the present study, the

successive dilatations provided information about the step-by-step disappearing speed of dark objects, which corresponded to the pores (serum and fat). Successive erosions provided information about the step-by-step disappearing speed of light objects, corresponding to the protein network. The images were processed using the program and the method of interpretation developed for cakes by Dewaest et al. (2017) using MatLab software (The MathWorks, France) and XLSTAT 2015.1 software (Addinsoft, Paris, France). A set of 183 confocal images [×40 magnification, 1 pixel = $(0.569)^2$ μm^2] obtained from 35 different recipes, including eight from the present study, were analysed to dispose of sufficient data for statistical interpretation and hence quantitative analysis of the microstructure.

The 80 total grey level values obtained from the 40 dilatations and 40 erosions of the 183 confocal images were analysed using principal component analysis (PCA). The position of each image in the PC1-PC2 plan was obtained. Using the PC1 and PC2 loadings of principal components plotted against micrometres, it was possible to interpret the microstructure of the confocal images. This provided information about object sizes ranging from 2.2 to 85.5 µm. In the present study, the pore size and the coarseness of protein network both changed according to the principal components PC1 and PC2. However, the diagonals (D1 and D2) made it possible to interpret the microstructure, and the coordinates of the confocal images on D1 and D2 were calculated.

2.6. Analysis of the texture using rheology and tribology taking oral processing into account

The texture was evaluated in conditions that took oral processing into account through shearing, temperature, and the small gaps chosen. The measurements were made by combining rheology and tribology, using the method developed by Huc, Michon, Bedoussac, and Bosc (2016). After a standardised mixing step, the sample was loaded onto the controlled Peltier plate of a MCR 301 rheometer (Anton Paar, Graz, Austria) set at 10 °C. Measurements were made using a plate-plate system (steel serrated parallel plate, 5 cm in diameter) with a gap of 1 mm and with an

increase in temperature from 10 °C to 25 °C, mimicking the increase in temperature that takes place in the mouth. The viscoelastic properties were first measured at 10 °C (0.01–10 Hz frequency, 0.1% strain chosen in the linear viscoelastic domain). In the second step, viscosity was measured at 60 s^{-1} while the temperature was increased from 10 °C to 18 °C (0.6 °C s^{-1} heating rate) and then the viscoelastic properties were measured at 25 °C (0.01–10 Hz frequency, 0.1% strain that was still in the linear viscoelastic domain) after 1 min at 25 °C under 60 s^{-1} shearing. Three replicate measurements were performed for each sample. Several indicators were chosen to describe the rheological properties: viscosity (η_0, Pa s) and storage moduli (G'_0, Pa, 1 Hz) at the beginning of the mimicked oral processing, viscosity (η_f, Pa s) and storage moduli (G'_f, Pa, 1 Hz) at the end of the mimicked oral processing, and changes in the properties during measurement through the ratios $R\eta$ (η_f / η_0) and RG' (G'_f / G'_0). In addition, friction was also measured using a nanotribometer NTR2 (CSM, Peseux, Switzerland) fitted with a polytetrafluoroethylene (PTFE) ball (2 mm in diameter) and a polydimethylsiloxane (PDMS) surface in contact. The temperature was set at 25 °C (Peltier control system). A sample 250 mm in height was loaded onto the PDMS and a 30 mN normal force load charge was applied with the PTFE ball sliding along a distance of 4 mm at a velocity of 10 mm s^{-1} for 15 cycles. The friction coefficient was calculated by dividing the friction tangential force measured (F_t) by the applied normal force (F_n) ($\mu = F_t / F_n$). At least five replicates were done per type of stirred milk gel. Only 10 cycles were retained for the evaluation of the friction coefficient, by averaging their values. Between each measurement, the surfaces were washed with ethanol and rinsed extensively with distilled water and then wiped dry.

2.7. Statistical analysis

Statistical analysis was performed using XLSTAT 2015.1 software (Addinsoft, Paris, France). Analysis of variance (ANOVA) was performed to evaluate differences between average values using Tuckey's test. Significance levels of $p \leq 0.05$ or $p \leq 0.1$ were used. Principal

component analysis (PCA) was used to analyse all the texture properties measured in instrumental conditions that mimicked oral processing.

3. Results and discussion

3.1. Thermal properties and sizes of fat droplets in the creams

Although the main sizes of fat droplets in the cream were generally similar (ranging from 1.4 µm to 2.1 µm), the fat droplets stabilised with native proteins were slightly smaller than the fat droplets stabilised with heat-aggregated proteins (Table 3). This difference in fat droplet sizes depending on the state of aggregation of the interfacial proteins has also been reported in the literature for emulsions made from rapeseed oil (3% fat) and whey protein concentrate (WPC) (3% protein) (Millqvist-Fureby, Elofsson, & Bergenståhl, 2001). This can be explained because once the proteins are heat-aggregated, they form fewer particles than when they are native and the amount of emulsifying material is consequently reduced. However, the results obtained by Truong et al. (2014) suggest that this difference in size was not sufficient to cause differences in fat droplet properties such as fat crystallisation. This result enabled to focus on the effects of the fat fraction and of interfacial proteins on the emulsion properties for the remainder of the present study.

As the differences in the composition of the creams were expected to impact their thermal properties, they were studied as a function of the type of fat and of the protein adsorbed at the interface (Fig. 2). The results showed that the melting profiles of the creams made from olein, AMF and stearin were different and all corresponded to wide melting ranges with one main melting peak (Fig. 2A). The three fat fractions started their melting between 0 °C and 5 °C and stopped around 11 °C for olein, 20–25 °C for AMF and 41 °C for stearin. This showed that olein was already melted at 8 °C whereas AMF melted during the increase in temperature from 8 °C to 25 °C (the temperature range representative of oral processing). Stearin only melted very slightly and remained mainly crystallised in this temperature range. The melting profiles also showed that there was no difference

due to the type of protein adsorbed at the interface (native or heat-aggregated). In addition, the SFC of cream calculated at 8 °C differed with the fat fraction (Fig. 2B). It was close to 0% for olein and between 45% and 50% for AMF. In the case of stearin, it varied significantly with the interface, with a value of 75% when the interfacial WPI was native and 50% when it was heat-aggregated. The composition of the fat thus had a major impact on the thermal properties of the tailored creams, whereas the type of protein adsorbed at the interface only influenced certain thermal properties (i.e., the SFC of the creams of stearin).

The melting profiles obtained for the creams made from the three fat fractions correspond to those expected and are in accordance with those reported in the literature for similar systems (Lopez et al., 2006; Truong, Morgan, Bansal, Palmer, & Bhandari, 2015). The SFC values obtained at 8 °C are also consistent with the values of 20%, 40% and 60% reported in the literature for olein, AMF and stearin emulsions, respectively (Lopez et al., 2006; Truong et al., 2015). These differences depending on the fat fractions can be linked to their fatty acid composition (Table 1). Indeed, the more unsaturated and the longer the fatty acids, the more difficult the crystallisation. Hence, at 8 °C, the fat crystals melted at lower temperature when the SFC was lower. Only one paper by Palanuwech and Coupland (2003) reported that crystallisation onset temperature increased when a cocoa butter emulsion was stabilised by heat-aggregated WPI (90 °C for 30 min) instead of native WPI, which is in accordance with the results obtained in the present study. In the case of the stearin droplets stabilised with heat-aggregated proteins, the increase in the onset crystallisation temperature coupled with the decrease in SFC, suggests that the protein aggregates contributed to the initiation of crystallisation, while limiting crystal growth by steric hindrance.

3.2. Rheological and lubrication properties of stirred milk gels

The different creams were used to make stirred milk gels and to evaluate the impact of the fat content, fat fraction and interfacial proteins on the properties of texture (G'_0, G'_f, η_0 and η_f) and lubrication (μ) of the stirred milk gels. The different properties were measured in conditions taking

328 oral processing into account and the results are listed in Table 4. First, the stirred milk gels were
329 similarly ranked according to their rheological properties and three groups differed, mainly
330 depending on their fat fraction and fat content. The first group consisted of the two olein stirred
331 milk gels [HTOL(6), OL(6)], with the lowest viscosities and storage moduli. The second group
332 consisted of the stirred milk gels with intermediate viscosities and storage moduli [AMF(6),
333 HTAMF(6), ST(6), HTST(6)]. The third group consisted of the stirred milk gels with the highest fat
334 content [AMF(10), HTAMF(10)], having the highest viscosities and storage moduli. In addition, the
335 viscosities and storage moduli of the stirred milk gels made from AMF tended to be higher when
336 the interfacial proteins were heat-aggregated. This effect was even more marked (and significant)
337 with a higher fat content.
338 The effect of the fat content observed is consistent with that already demonstrated for stirred
339 yoghurts (Krzeminski, Großhable, & Hinrichs, 2011). The protein-stabilised fat droplets are fillers
340 known to contribute to the protein network thus explaining the reinforcement of the rheological
341 properties of the stirred milk gel when its fat content is increased (10% instead of 6%). In addition,
342 the literature reported that the fat fraction and interfacial proteins also had an impact on the stiffness
343 of emulsion-filled gels (Liu et al., 2015; Oliver et al., 2015; Sala et al., 2007) and set milk gels (Cho
344 et al., 1999; Houzé et al., 2005). To the best of our knowledge, this impact has not yet been
345 demonstrated for stirred systems. However, it has been reported that the viscosity of concentrated
346 dispersions was higher when the particles were stiffer (Barnes, 2000). The results obtained in the
347 present study can thus be interpreted by assuming that the stiffer the initial set milk gel, the stiffer
348 its microgels after stirring, and consequently the higher the viscosity and the storage modulus of the
349 stirred milk gel. Some authors reported that an increase in the droplet solid fat content increased the
350 fat droplet hardness and hence the stiffness of the emulsion-filled gel (Liu et al., 2015; Oliver et al.,
351 2015). In the present study, it can thus be assumed that the olein stirred milk gels had the lowest
352 viscosities and storage moduli because their droplets were liquid at 10 °C and 25 °C, in contrast to
353 the AMF and stearin stirred milk gels (whose droplets were at least partly crystallised).

Furthermore, Cho et al. (1999) reported an increase in viscosity and storage modulus when the interfacial proteins were heat-aggregated, and the results shown in Table 4 are in good agreement with their results. Liu et al. (2015) and Sala et al. (2007) reported that stronger interactions between the dispersed and continuous phases tended to increase the stiffness of emulsion-filled gels. In the present study, it can thus be assumed that the fat droplets interacted more with the protein network when the interfacial WPI were heat-aggregated. Since we demonstrated in a previous work that heat-induced WPI aggregates are bigger and more hydrophobic than native ones (Moussier et al., 2019a), the increased interactions between the protein interface and the protein network were probably due to more hydrophobic interactions (Nguyen, Wong, Guyomarc'h, Havea, & Anema, 2014) and/or stronger mechanical anchoring. In the specific case of stearin, Truong et al. (2015) showed the droplets to be irregular in shape due to the formation of large fat crystals. This may have reduced the interaction between the stearin droplets and the protein network (spatial hindrance), thus limiting the "strengthening" effect of the interfacial heat-aggregated WPI. With olein, the fat droplets were liquid and the effect of the strengthening interface was probably offset, underlining the combined effect of the interface and fat compositions.

Changes in the rheological properties after the temperature was increased from 10 °C to 25 °C (under 60 s^{-1} shearing) were measured using the parameters RG' and Rη (Table 4), which tended towards 0 when the properties varied strongly along the measurement, and towards 1 when they varied only slightly. The stirred milk gels were similarly ranked based on RG' and on Rη, resulting in three main groups that depended mainly on the fat fraction. The RG' and Rη values of stirred milk gels were the lowest with AMF, intermediate with stearin and the highest with olein. In the case of the stirred milk gels made from AMF, the Rη values were even lower for a higher fat content. It was demonstrated in Subsection 3.1 that AMF melted completely between 10 °C and 25 °C, whereas the states of stearin (remaining crystallised) and olein (already almost completely

melted) did not change much in this temperature range. The differences in RG' and Rη obtained can thus be linked to the thermal properties of the fat fractions.

The friction coefficient (μ) was measured at 25 °C and made it possible to distinguish the stirred milk gels made from stearin (ST(6), HTST(6)) whose μ was significantly higher, from all the other stirred milk gels (Table 4). Several authors demonstrated that the friction coefficient decreased when an oily film was formed after the coalescence of the fat droplets at small gap friction (Chojnicka-Paszun, de Jongh, & de Kruif, 2012). Since stearin was mainly crystallised at 25 °C, it may not have formed the lubricating oily film, resulting in a higher friction coefficient than with olein and AMF, both of which were completely melted at 25 °C. This effect was strengthened when interfacial WPI was heat-aggregated, probably because the resulting thicker interfacial film was even more resistant to coalescence under shearing in a very small gap.

3.3. Structural properties of stirred milk gels

The microgel median diameters of the stirred milk gels ranged from 11 µm to 21 µm depending on the fat content and on the state of proteins adsorbed at the interface (Table 5). The microgels were smaller when the fat droplet interface was composed of heat-aggregated WPI and when the stirred milk gel contained more fat (i.e., 10 wt%). However, there was no significant effect of the type of fat on the size of the stirred milk microgels.

The order of magnitude of the microgel sizes obtained was close to the sizes reported in the literature (Abhyankar, Mulvihill, & Auty, 2014). These results show that stirring resulted in smaller microgels when the texture of the set gel obtained after acidification was strengthened by parameters such as fat content or heat-aggregated WPI at the interface. This is consistent with literature reporting that model emulsion-filled gels were more brittle under stirring if they were stiffer, breaking down into smaller pieces (Chojnicka, Sala, de Kruif, & van de Velde, 2009). Knowing that tailoring the cream affected the stirred milk microgels, it was then decided to analyse

in more detail how the proteins, fat droplets and serum were structured in the stirred milk gel matrices.

All the micrographs in Fig. 3 show a protein network (in green), in which the microgels are not visible individually, dispersed fat (in red), serum-filled pores (in black) and fat-protein co-location zones (in yellowish-orange). In all of the micrographs, the fat droplets are aggregated with some yellowish-orange zones typical of dispersed fat stabilised by proteins. The fat droplet aggregates are either separate entities such as microgels (10–20 µm, arrow 2 in Fig. 3) or are embedded in the global protein network (arrow 3 in Fig. 3). The structures are typical of model emulsion-filled gels (Liu et al., 2015) and of stirred yoghurts (Huc et al., 2016) described in the literature. There are no visible differences between the micrographs depending on fat fractions (AMF, stearin and olein), and all the micrographs are similar with respect to the distribution of fat droplet aggregates. However, the global protein networks of the stirred milk gels containing more fat or aggregated WPI at the interface appeared to be thinner and less porous. A quantitative analysis was then performed using mathematical morphology to provide an objective basis for the structure and to quantify the differences (Fig. 4).

The mathematical morphology analysis was performed using the confocal images of the global protein network only, with fat appearing as dark objects (as did serum-filled pores). A 2D score plot (PC1, PC2) was selected from the PCA of the grey level sums (for all dilatations and erosions) obtained using mathematical morphology (Fig. 4A). The corresponding score plot displays more than 73% of the total information and the stirred milk gel micrographs used for mathematical morphology are well distributed on it, indicating a diversity of the microstructures. The analysis of the PC1 and PC2 loadings (Fig. 4C) provided interpretations of the axes with respect to the sizes of dark objects (i.e., pores) and light objects (i.e., the protein network). According to these size interpretations, both the dark and light object sizes varied simultaneously on the PC1 and PC2 axes. However, the diagonals D1 and D2 made it possible to distinguish the sizes of the dark and light objects, thereby facilitating the interpretation about the microstructure. Among

all the points on the PC1-PC2 mapping, the most discriminating ones (at the extremities) were chosen to interpret D1 and D2 axes (*a*, *b*, *c*, *d*, *e*). The confocal images corresponding to the *a*, *b*, *c*, *d*, and *e* points display different microstructures (Fig. 4B). As was the case in Fig. 3, the microgels are not visible on any of the confocal images. The images *a* and *b* show a very thin protein network and small pores, whereas image *d* shows a coarse protein network and large pores. In between, images *c* and *e* both display a quite thin protein network (locally), with small pores in *c* and larger ones in *e*. Based on these discriminating confocal images and the sizes obtained from the loadings, D1 was identified as an axis representing the coarseness of protein network (from thin to coarse) and D2 the size of the pore (from small to large). This quantitative interpretation of the microstructure is similar to the levels of organisation that Mellema, Walstra, van Opheusden, and van Vliet (2002) described for skim milk gels (through aggregation and microsyneresis/pores).

All the points of the PC1-PC2 mapping corresponding to the stirred milk gels in the present study (black ellipse in Fig. 4A) were projected on the D1 and D2 diagonals and their coordinates were collected. The average and standard deviation of the D1 and D2 scores were then calculated for each stirred milk gel (Fig. 5). The D1 scores (Fig. 5A) had larger standard deviations than D2 scores (Fig. 5B), meaning greater variability of the images for a given stirred milk gel from the point of view of the coarseness of the protein network. However, the D1 scores differed more from one stirred milk gel to another and were therefore easier to interpret than D2 scores, for which smaller variations were observed. The high standard deviations of the scores can be explained by the variability when the confocal images were taken. High variability of scores is quite common in mathematical morphology but they nevertheless make it possible to identify trends and to quantitatively interpret the microstructure (Dewaest et al., 2017; Fenoul et al., 2008).

The protein network coarseness displayed no clear trend (D1, Fig. 5A) based on fat content. However, the protein networks were globally thinner when the interfacial proteins were heat-aggregated WPI. This effect was even stronger for stirred milk gels made from stearin and olein [HTST(6) < ST(6) and HTOL(6) < OL(6)]. Although not statistically significant, the pores (D2

scores, Fig. 5B), were slightly larger when the fat content was higher. This makes sense, because fat was not taken into account in mathematical morphology analysis, and therefore appeared as pores (in black) on the confocal images. In addition, at the same fat content, the pores in stirred milk gels having heat-aggregated WPI at the interface were larger with olein and AMF [OL(6) < HTOL(6) and AMF(6) < HTAMF(6)] but smaller with stearin [HTST(6) < ST(6)].

These quantitative results indicate that heat-aggregated WPI increased the interactions within the matrix, leading to thinner networks. They confirm our qualitative analysis of the confocal images of the stirred milk gels (Fig. 3). The larger pores quantified for olein and AMF suggest greater syneresis (Mellema et al., 2002; Renan et al., 2009) in the presence of heat-aggregated WPI at the interface, probably due to the stronger interactions in the matrix (via the interface) (Cho et al., 1999). In the case of stearin, this effect was not confirmed. It was shown in Subsection 3.1 (Fig. 2) that the stearin droplet SFC was not the same if the interfacial proteins were native (SFC of 75%) or heat-aggregated (SFC of 50%). Fredrick, Walstra, and Dewettinck (2010) reported an optimum SFC between 20% and 50%, at which partial coalescence is promoted and above which partial coalescence is much less likely. Palanuwech and Coupland (2003) also demonstrated that emulsion destabilisation (partial and total coalescence) was possible with aggregated WPI at the interface. In the present study, it is likely that interactions between stearin droplets were enhanced when the interfacial proteins were aggregated WPI through easier partial coalescence, limiting interactions with the protein network and therefore syneresis (i.e., larger pores). It was showed in Subsection 3.1 that the SFC of the AMF droplets stabilised either with native or heat-aggregated proteins was around 50%. Based on the literature (Fredrick et al., 2010; Palanuwech & Coupland, 2003), we expected the partial coalescence of the AMF droplets to be similar to that assumed for stearin droplets stabilised with heat-aggregated WPI, but this was not the case. This result suggests that the types of crystals formed with AMF and stearin were not the same, resulting in different partial coalescence of the droplets.

3.4. Relationship between the stirred milk gel formulation and their structural and textural properties

The variables measured at the different scales were analysed together to see if (and how) they were correlated, and to what extent tailoring the cream made it possible to produce different stirred milk gels. A previous correlation test showed that properties G'_0, G'_f, η_0 and η_f, as well as properties RG' and Rη, were correlated. The properties G' and RG' were therefore selected among all the rheological properties. The previous correlation test also showed that the microgel median size determined by laser diffraction [d(0.5) µgels] and the coarseness of the protein network determined by mathematical morphology (D1) were correlated. This correlation indicated that the thinner the protein network, the smaller the microgels. The properties D2 and d(0.5) µgels were thus selected as the microstructure indicators for this multi-scale analysis.

The principal component analysis (PCA) plotted in Fig. 6 gives a mapping of the stirred milk gels as a function of all the chosen variables. The selected 2D projection (F1; F2) displays 73% of the total information. According to the correlation loading plot (Fig. 6A), the F1 axis explains more than 44% of the total information and displays the rheological properties (G'_0 and RG'), SFC (8°C) and d(0.5) µgels. The F2 axis explains almost 29% of the total information through µ(25°C) and D2. Overall, the variables are distributed all around the correlation loading plots, indicating that the studied properties were complementary.

Based on the table listing the Pearson's correlation coefficients (Table 6), G'_0 and RG' were anti-correlated, meaning that the higher the storage modulus of the stirred milk gels, the bigger the decrease in the storage modulus in conditions that account for oral processing. Moreover, the friction coefficient was not correlated with the rheological properties. The two measurement are complementary in characterising stirred milk gels, as already shown by Huc et al. (2016). Regarding structural properties, no correlation was found between microgel size [d(0.5 µgels] and pore size (D2). This result indicates that the pore size obtained by mathematical morphology is

complementary to the microgel size and that there is no direct relationship between these two structural indicators. In addition, Pearson's correlation coefficients revealed different links between the structural and textural (lubrication and rheology) properties. In particular, μ(25°C) was slightly correlated with SFC(8°C) and anti-correlated with D2. G'_0 was correlated with SFC(8°C) and anti-correlated with d(0.5) μgels. Conversely, RG' was highly anti-correlated with SFC(8°C) and correlated with d(0.5) μgels.

Furthermore, the samples are well distributed on the score plot in Fig. 6B, indicating that a range of stirred milk gels with different properties was produced by tailoring cream. Different groups can be defined according to both F1 and F2, depending on fat fraction (AMF, olein or stearin), interface (native or heat-aggregated WPI) and fat content (6 or 10% fat). The stirred milk gels made from olein or containing more fat differed from the other samples on the F1 axis, depending on the rheological properties, the SFC and the size of the microgels. These gels had a small G'_0, a small SFC and a high RG' (i.e., small changes in G' between 8 and 25 °C). On the F2 axis, the stirred milk gels made from stearin differed from the other samples, with a high level of μ(25°C) and small pore size (D2). The stirred milk gels made from AMF all had the same SFC(8°C) but different G'_0 depending on the interface and the fat content: heat-aggregated or a higher fat content led to smaller μ(25°C) and higher G'_0.

The structural parameters and the measured textural properties thus proved to be complementary for the characterisation of the stirred milk gels obtained by tailoring the formulation via the fat content, the state of the interfacial protein and the fat composition. The relationship between formulation, structure and texture shown here for realistic dispersions of emulsion-filled microgels, contributes additional results to the literature, in which this relationship has only been shown for model systems up to now (Chojnicka et al., 2009; Liu et al., 2015; Oliver et al., 2015).

The resulting effects at different scales are summarised in Fig. 7. First, the change in the fat fraction mainly modified the thermal properties (both melting and SFC), and these modifications affected the final properties of the stirred milk gels at different levels. Still strongly crystallised at

25 °C, stearin generated the highest friction coefficients of the stirred milk gels. As olein was already melted and liquid at 10 °C, it led to the lowest rheological properties. The rheological properties of the stirred yoghurts made with olein and stearin changed little between 8 and 25 °C (i.e., high values of RG'), certainly due to the small variations in the SFCs of these two types of fat over this temperature range. By melting between 10 °C and 25 °C, AMF caused the biggest changes in the rheological properties (i.e., lowest RG') in this temperature range. The interface mainly impacted the coarseness of the protein network and the size of the microgels. The heat-aggregated WPI (at the interface) likely increased interactions of the fat droplets among themselves (within the droplet aggregates) and with the protein network (when embedded in the network). This increase in interactions probably strengthened the structure and enhanced its stiffness, which certainly increased its brittleness during stirring and consequently led to smaller microgels (Chojnicka et al., 2009). The small microgels tended to increase the stiffness of stirred milk gels, which may be due to improved homogeneity of the microgels, as shown by Hahn et al. (2015) for stirred milk gels. Finally, big pores tended to decrease friction coefficient, certainly because of the presence of larger amount of serum surrounding the stirred-milk microgels. In the specific case of stearin, the in-depth study of the microstructure suggested that droplets increased their partial coalescence when interfacial WPI were heat-aggregated instead of native (due to a more suitable SFC) and this may also explain the slight increase in the friction coefficient then measured. Regarding olein, the droplets were liquid and certainly poorly texturising, which offset the strengthening effect of heat-aggregated WPI (at the interface). The study thus highlighted that the interface and fat fraction had a combined effect on the stirred milk gel properties.

4. Conclusions

While emulsion-filled gels are relatively well analysed in the literature, the dispersions of emulsion-filled microgels obtained after stirring have rarely been studied. The aim of the present

study was to measure the effects of tailoring the fat fraction (AMF, olein or stearin) and interfacial protein (native or heat-aggregated WPI) of the fat droplets (in cream) on the properties of stirred milk gels. By using a multi-scale approach, this work clearly demonstrated the existence of a relationship between formulation, the structural and macroscopic properties of stirred milk gels. It provided new interpretations that highlight some structuring mechanisms of this complex system, depending on both the fat fraction and the interface. In particular, the present study has shown that crystallised fat droplets can reinforce the texture whereas liquid droplets tended to weaken it. The level of interactions between the interface and the protein network can be driven by the type of the adsorbed proteins and can modify both the thinness of the protein network and the rheological properties of the stirred milk gel. In addition, small microgels may have been formed when the protein network was thinner, likely because they were less deformable when stirred. As the stirred milk gels were realistically formulated and characterised in conditions that took oral processing (temperature increase under constant shearing) into account, this study suggest that tailoring cream would modify sensory properties and provide interesting levers for future innovations.

Acknowledgements

This work was funded by a single interministerial fund (France) through a collaborative R&D project certified by Vitagora and Valorial competitiveness clusters. The authors would like to thank Mélanie Ngo, Morgane Tertre and Congcong Jiang for their contribution to the stirred milk gels and measurements. The authors also thank Marie-Noëlle Maillard for her expertise and the time she devoted to the presentation and measurement of fatty acid compositions (chromatography coupled to mass spectrometry) and Gabrielle Moulin for sharing her experience and spending time measuring microstructures (confocal laser scanning microscopy).

References

Abhyankar, A. R., Mulvihill, D. M., & Auty, M. A. E. (2014). Combined confocal microscopy and large deformation analysis of emulsion filled gels and stirred acid milk gels. *Food Structure*, *1*, 127–136.

Barnes, H. A. (2000). *A handbook of elementary rheology*. Aberystwyth, Swansea and Cardiff, Wales: The University of Wales Institute of Non-Newtonian Fluid Mechanics.

Barrantes, E., Tamine, A. Y., Sword, A. M., Muir, D. D., & Kalàb, M. (1996). The manufacture of set-type natural yoghurt containing different oils. 2. Rheological properties and microstructure. *International Dairy Journal*, *6*, 827–837.

Cano-Ruiz, M. E., & Richter, R. L. (1997). Effect of homogenization pressure on the milk fat globule membrane proteins. *Journal of Dairy Science*, *80*, 2732–2739.

Cayot, P., & Lorient, D. (1998). *Structures et technofonctions des protéines du lait* (TEC & DOC). Paris, France: Lavoisier.

Cho, Y. H., Lucey, J. A., & Singh, H. (1999). Rheological properties of acid milk gels as affected by the nature of the fat globule surface material and heat treatment of milk. *International Dairy Journal*, *9*, 537–545.

Chojnicka-Paszun, A., de Jongh, H. H. J., & de Kruif, C. G. (2012). Sensory perception and lubrication properties of milk: Influence of fat content. *International Dairy Journal*, *26*, 15–22.

Chojnicka, A., Sala, G., de Kruif, C. G., & van de Velde, F. (2009). The interactions between oil droplets and gel matrix affect the lubrication properties of sheared emulsion-filled gels. *Food Hydrocolloids*, *23*, 1038–1046.

Dewaest, M., Villemejane, C., Berland, S., Clément, J., Aliette, V., & Michon, C. (2017). Effect of crumb cellular structure characterized by image analysis on cake softness. *Journal of Texture Studies*, 1–11.

612 Donato, L., & Guyomarc'h, F. (2009). Formation and properties of the whey protein/kappa-casein
613 complexes in heated skim milk - A review. *Dairy Science and Technology*, *89*, 3–29.
614 Fenoul, F., Le Denmat, M., Hamdi, F., Cuvelier, G., & Michon, C. (2008). Technical note:
615 Confocal scanning laser microscopy and quantitative image analysis: Application to cream
616 cheese microstructure investigation. *Journal of Dairy Science*, *91*, 1325–1333.
617 Fredrick, E., Walstra, P., & Dewettinck, K. (2010). Factors governing partial coalescence in oil-in-
618 water emulsions. *Advances in Colloid and Interface Science*, *153*, 30–42.
619 Hahn, C., Nöbel, S., Maisch, R., Rösingh, W., Weiss, J., & Hinrichs, J. (2015). Adjusting
620 rheological properties of concentrated microgel suspensions by particle size distribution.
621 *Food Hydrocolloids*, *49*, 183–191.
622 Houzé, G., Cases, E., Colas, B., & Cayot, P. (2005). Viscoelastic properties of acid milk gel as
623 affected by fat nature at low level. *International Dairy Journal*, *15*, 1006–1016.
624 Huc, D., Michon, C., Bedoussac, C., & Bosc, V. (2016). Design of a multi-scale texture study of
625 yoghurts using rheology, and tribology mimicking the eating process and microstructure
626 characterisation. *International Dairy Journal*, *61*, 126–134.
627 Krzeminski, A., Großhable, K., & Hinrichs, J. (2011). Structural properties of stirred yoghurt as
628 influenced by whey proteins. *LWT - Food Science and Technology*, *44*, 2134–2140.
629 Le Calvé, B., Saint-Léger, C., Babas, R., Gelin, J.-L., Parker, A., Erni, P., & Cayeux, I. (2015). Fat
630 perception: How sensitive are we? *Journal of Texture Studies*, *46*, 200–211.
631 Lee, W. J., & Lucey, J. A. (2010). Formation and physical properties of yogurt. *Asian-Australasian*
632 *Journal of Animal Sciences*, *23*, 1127–1136.
633 Liu, K., Stieger, M., van der Linden, E., & van de Velde, F. (2015). Fat droplet characteristics affect
634 rheological, tribological and sensory properties of food gels. *Food Hydrocolloids*, *44*, 244–
635 259.
636 Lopez, C., Briard-Bion, V., Camier, B., & Gassi, J.-Y. (2006). Milk fat thermal properties and solid
637 fat content in Emmental cheese: A differential scanning calorimetry study. *Journal of Dairy*

638 *Science*, *89*, 2894–2910.
639 Lopez, C., Briard-Bion, V., & Ménard, O. (2014). Polar lipids, sphingomyelin and long-chain
640 unsaturated fatty acids from the milk fat globule membrane are increased in milks produced
641 by cows fed fresh pasture based diet during spring. *Food Research International*, *58*, 59–68.
642 Lucey, J. A., Munro, P. A., & Singh, H. (1998). Rheological properties and microstructure of acid
643 milk gels as affected by fat content and heat treatment. *Journal of Food Science*, *63*, 660–
644 664.
645 Mellema, M., Walstra, P., van Opheusden, J. H. J., & van Vliet, T. (2002). Effects of structural
646 rearrangements on the rheology of rennet- induced casein particle gels. *Advances in Colloid*
647 *and Interface Science*, *98*, 25–50.
648 Michalski, M. C., Cariou, R., Michel, F., & Garnier, C. (2002). Native vs. damaged milk Fat
649 globules: Membrane properties affect the viscoelasticity of milk gels. *Journal of Dairy*
650 *Science*, *85*, 2451–2461.
651 Millqvist-Fureby, A., Elofsson, U., & Bergenståhl, B. (2001). Surface composition of spray-dried
652 milk protein-stabilised emulsions in relation to pre-heat treatment of proteins. *Colloids and*
653 *Surfaces B: Biointerfaces*, *21*, 47–58.
654 Moussier, M., Bosc, V., Michon, C., Pistre, V., Chaudemanche, C., & Huc-Mathis, D. (2019a).
655 Multi-scale understanding of the effects of the solvent and process on whey protein
656 emulsifying properties : Application to dairy emulsion. *Food Hydrocolloids*, *87*, 869–879.
657 Moussier, M., Huc-Mathis, D., Michon, C., & Bosc, V. (2019b). Rational design of a versatile lab-
658 scale stirred milk gel using a reverse engineering logic based on microstructure and textural
659 properties. *Journal of Food Engineering*, *249*, 1–8.
660 Nguyen, N. H. A., Wong, M., Guyomarc'h, F., Havea, P., & Anema, S. G. (2014). Effects of non-
661 covalent interactions between the milk proteins on the rheological properties of acid gels.
662 *International Dairy Journal*, *37*, 57–63.
663 Oliver, L., Scholten, E., & van Aken, G. A. (2015). Effect of fat hardness on large deformation

rheology of emulsion-filled gels. *Food Hydrocolloids*, *43*, 299–310.

Palanuwech, J., & Coupland, J. N. (2003). Effect of surfactant type on the stability of oil-in-water emulsions to dispersed phase crystallization. *Colloids and Surfaces A: Physicochemical and Engineering Aspects*, *223*, 251–262.

Renan, M., Guyomarc, F., Arnoult-Delest, V., D, P., Brulé, G., & Famelart, M. H. (2009). Rheological properties of stirred yoghurt as affected by gel pH on stirring, storage temperature and pH changes after stirring. *International Dairy Journal*, *19*, 142–148.

Sala, G., van Aken, G. A., Stuart, M. A. C., & van de Velde, F. (2007). Effect of droplet-matrix interactions on large deformation properties of emulsion-filled gels. *Journal of Texture Studies*, *38*, 511–535.

Sodini, I., Remeuf, F., Haddad, S., & Corrieu, G. (2004). The relative effect of milk base, starter, and process on yogurt texture: A review. *Critical Reviews in Food Science and Nutrition*, *44*, 113–137.

Tomaschunas, M., Hinrichs, J., Köhn, E., & Busch-Stockfisch, M. (2012). Effects of casein-to-whey protein ratio, fat and protein content on sensory properties of stirred yoghurt. *International Dairy Journal*, *26*.

Truong, T., Bansal, N., Sharma, R., Palmer, M., & Bhandari, B. (2014). Effects of emulsion droplet sizes on the crystallisation of milk fat. *Food Chemistry*, *145*, 725–735.

Truong, T., Morgan, G. P., Bansal, N., Palmer, M., & Bhandari, B. (2015). Crystal structures and morphologies of fractionated milk fat in nanoemulsions. *Food Chemistry*, *171*, 157–167.

Figure legends

Fig. 1. Cooling and heating kinetics used to study the crystallisation (grey lines) and fusion (black lines) properties of milk fats with cooling either to –55 °C (solid line) or to 8 and then to –10 °C (dotted line).

Fig. 2. Average enthalpy profiles (A) during the melting (heating at 2 °C min^{-1}) of creams (60 wt% fat) cooled at 8 °C (–10 °C), with stearin (ST), AMF or olein (OL) and stabilised either with native WPI (dashed line) or with heat-aggregated (HT) ones (solid line). The range of temperature mimicking oral processing (between 25 and 8 °C) is indicated with a pale grey rectangle. Solid fat content (8 °C; B) of fat emulsified either with native (pale grey) or with heat-aggregated WPI (dark grey).

Fig. 3. Images of the different types of stirred milk gels obtained by CLSM; magnification 40×; scale bar = 50 µm. Fat droplets are shown in red, the global protein network in green, areas where proteins and fat are co-located are yellowish-orange (arrow 1) and areas containing only serum are black. There are highly aggregated fat droplets in the serum (arrow 2) and embedded in the protein matrix (arrow 3).

Fig. 4. Mathematical morphology analysis of the protein organisation at microscopic scale: PC1-PC2 mapping (A) of stirred milk gels obtained from the PCA and the confocal images, with the ellipse (black line) outlining the area where the stirred milk gels studied in this work are located on the map; samples *a* to *e* illustrate the axes (B); loadings of PC1 and PC2 versus micrometres of the size of the structuring element transformation (C) (more details on erosions, dilatations and mathematical morphology are given in subsection 2.5.2.).

Fig. 5. D1 scores (A; coarseness of the protein network) and D2 scores (B; size of the pores) from the mathematical morphology analysis of the stirred milk gel confocal images.

Fig. 6. Correlation loading plot (A) of the functional properties [G'_0, RG', μ (25 °C)], microstructure indicators [median diameter of the microgels d(0.5) μgels, pore size D2] and solid fat content at 8 °C [SFC (8 °C)] and score plot (B) of the different types of stirred milk gels produced.

Fig. 7. Diagram showing the relationship between the formulation, structure and texture of 6 wt% fat stirred milk gels (the effect of fat increase being better known). Different creams tailored in terms of fat fraction (AMF, olein or stearin) and interfacial proteins (native or heat-aggregated WPI) led to different thermal properties (SFC at 8 °C) and different stirred milk gel structures (pore size, microgel size, protein network coarseness, interactions of the fat droplets between themselves or with the protein network). All these differences resulted in different textural and lubrication properties (G'_0, RG' and μ) of the stirred milk gels measured in conditions that accounted for oral processing.

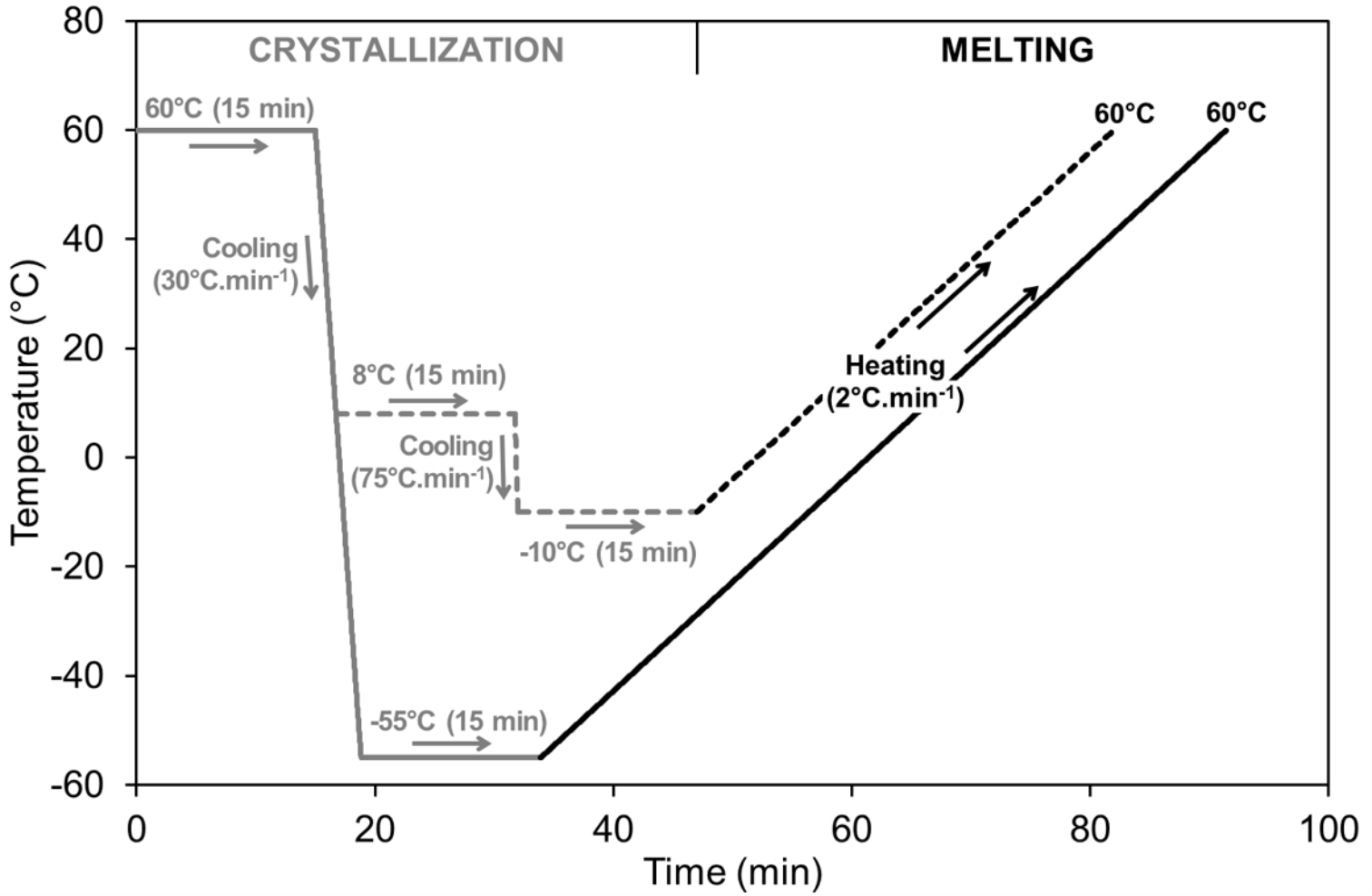
CRYSTALLIZATION
MELTING
60°C (15 min)
Cooling
(30°C.min-1)
8°C (15 min)
Cooling
(75°C.min-1)
-10°C (15 min)
-55°C (15 min)
Heating
(2°C.min-1)
60°C
60°C
Temperature (°C)
Time (min)
80
60
40
20
0
-20
-40
-60
0
20
40
60
80
100

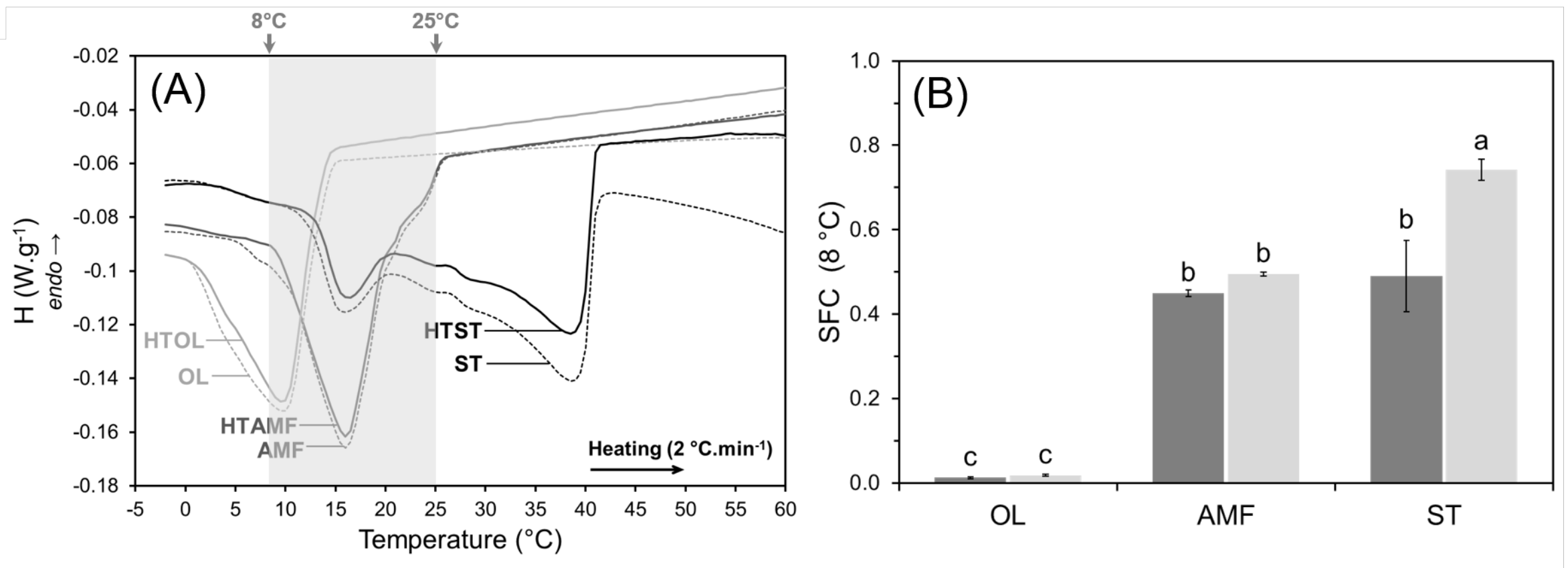
8°C
25°C
(A)
H (W.g-1)
endo →
-0.02
-0.04
-0.06
-0.08
-0.1
-0.12
-0.14
-0.16
-0.18
HTOL
OL
HTAMF
AMF
HTST
ST
Heating (2 °C.min-1)
-5 0 5 10 15 20 25 30 35 40 45 50 55 60
Temperature (°C)
(B)
SFC (8 °C)
1.0
0.8
0.6
0.4
0.2
0.0
c c
b b
b
a
OL
AMF
ST

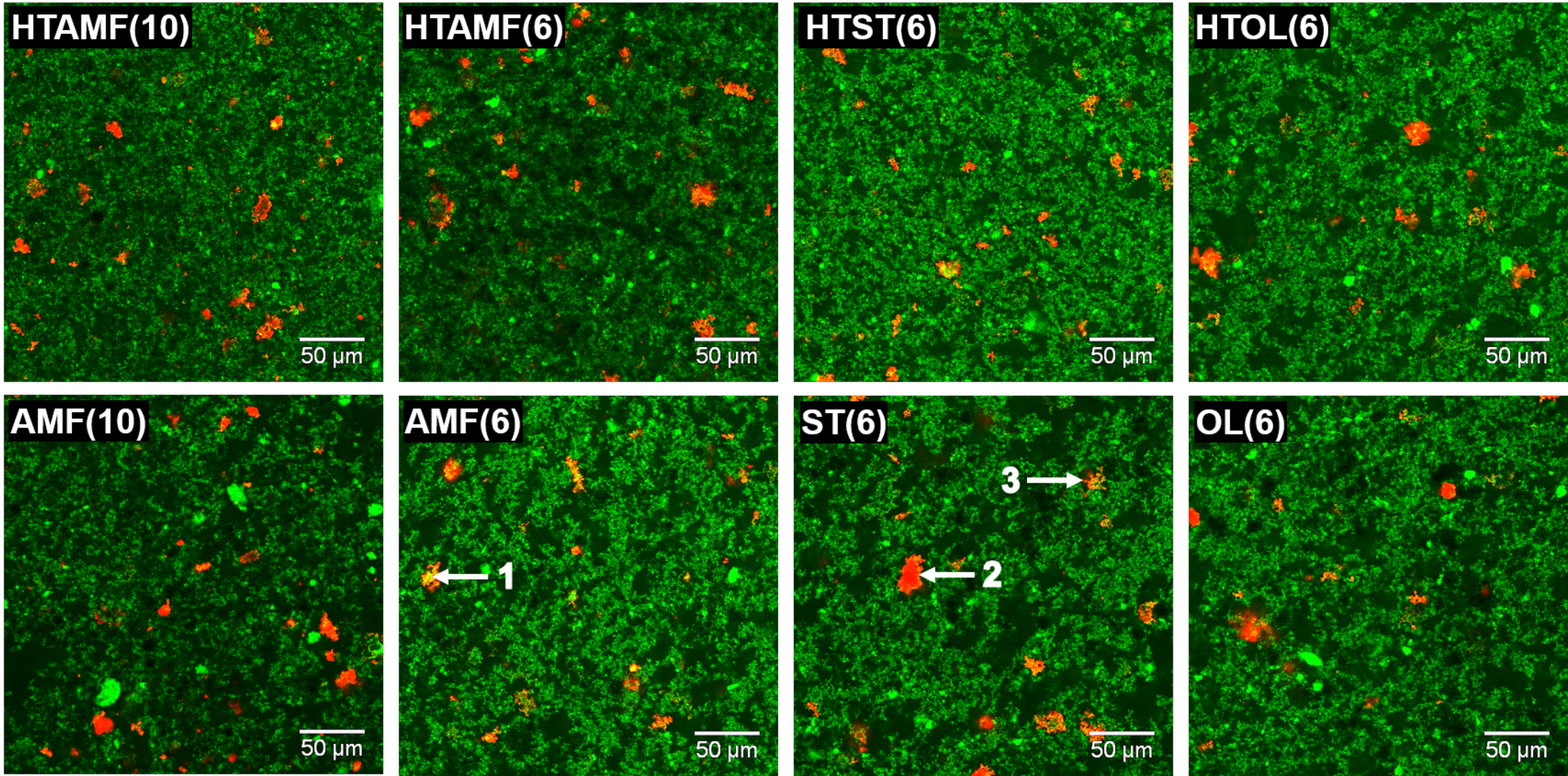
HTAMF(10)
HTAMF(6)
HTST(6)
HTOL(6)
AMF(10)
AMF(6)
ST(6)
OL(6)
50 µm
1
2
3

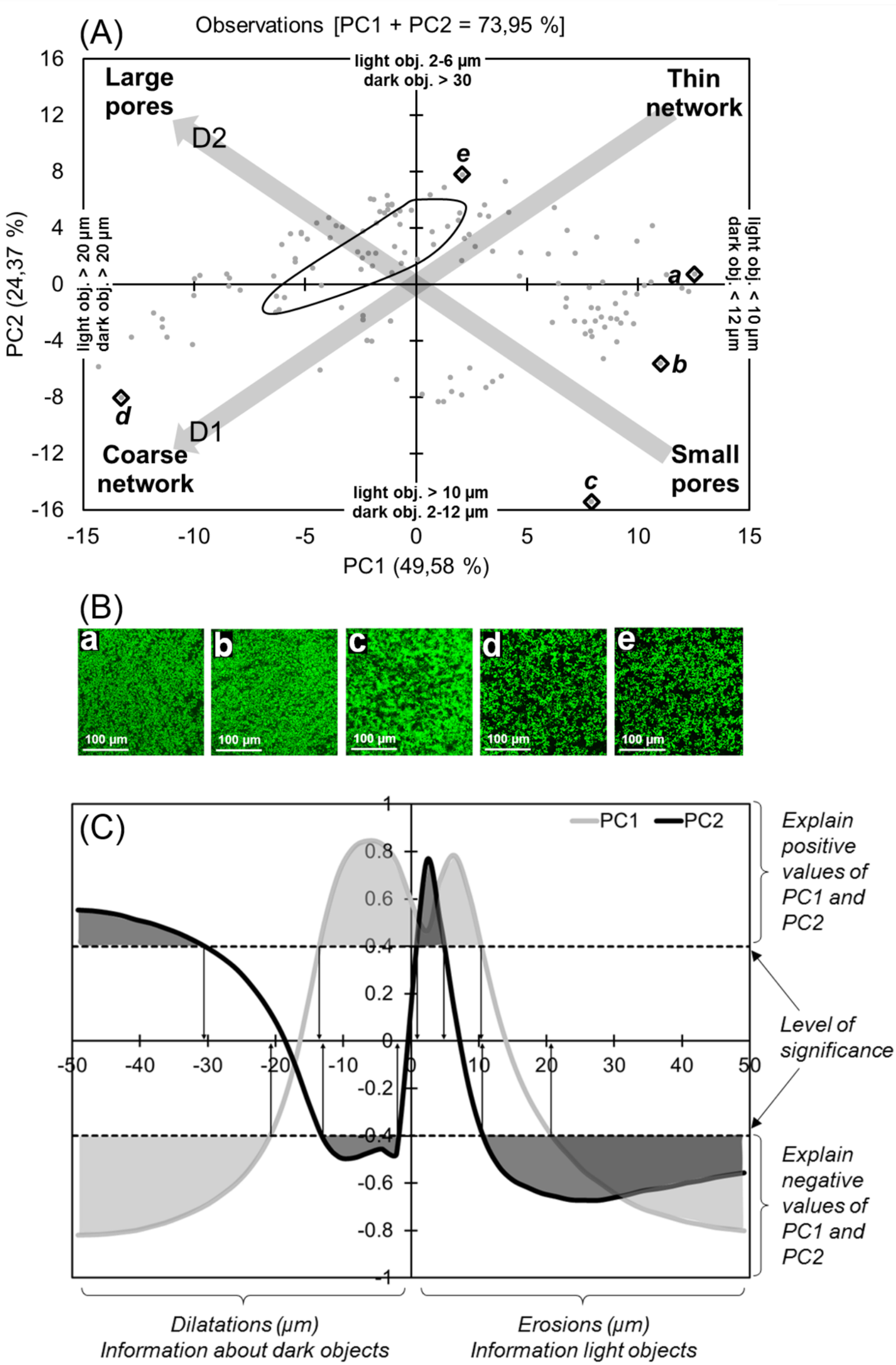
(A)
Observations [PC1 + PC2 = 73,95 %]
light obj. 2-6 µm
dark obj. > 30
Large pores
Thin network
D2
e
a
b
d
D1
Coarse network
Small pores
c
light obj. > 10 µm
dark obj. 2-12 µm
light obj. > 20 µm
dark obj. > 20 µm
light obj. < 10 µm
dark obj. < 12 µm
PC2 (24,37 %)
PC1 (49,58 %)
(B)
a
b
c
d
e
100 µm
(C)
PC1
PC2
Explain positive values of PC1 and PC2
Level of significance
Explain negative values of PC1 and PC2
Dilatations (µm)
Information about dark objects
Erosions (µm)
Information light objects

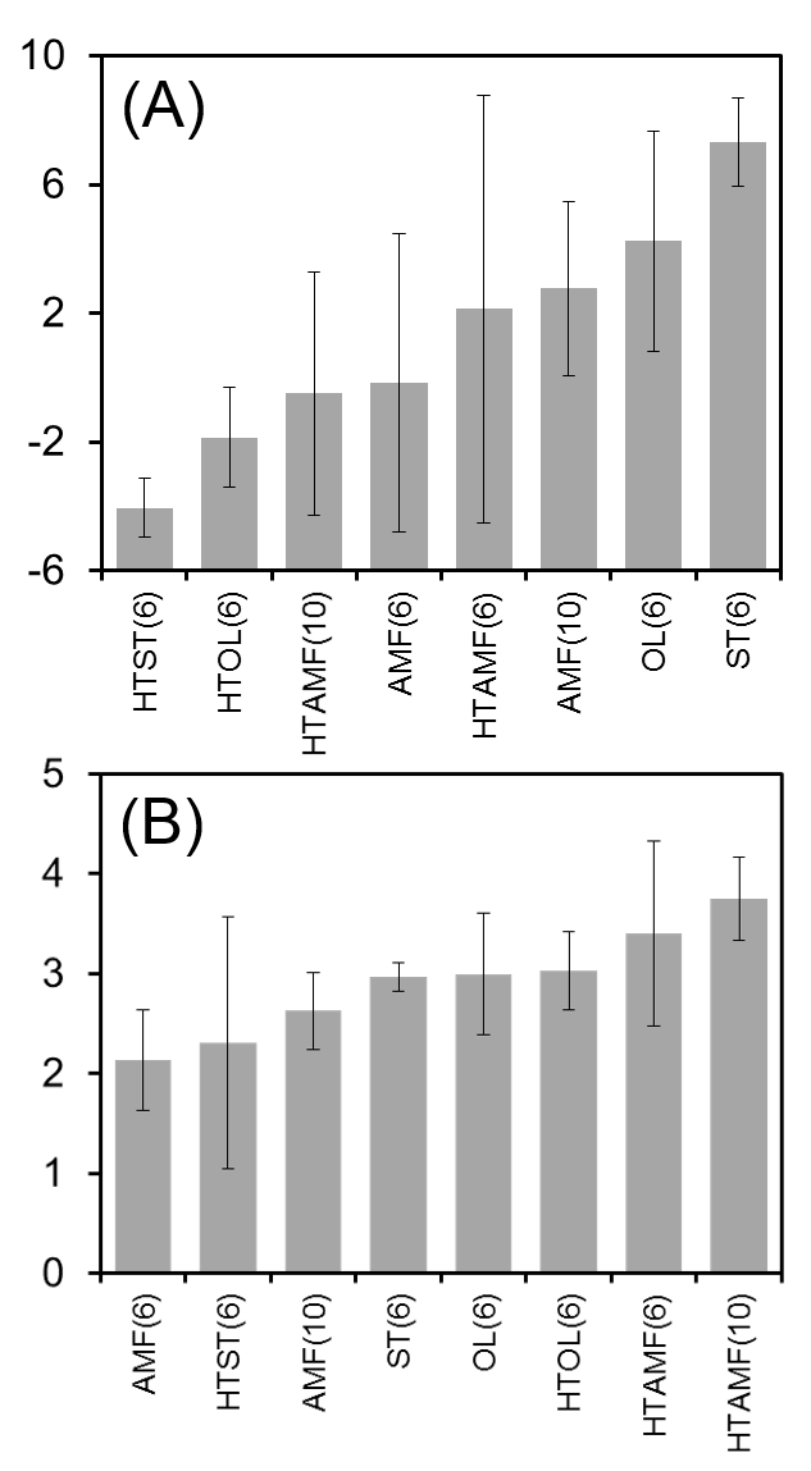
(A)
10
6
2
-2
-6
HTST(6)
HTOL(6)
HTAMF(10)
AMF(6)
HTAMF(6)
AMF(10)
OL(6)
ST(6)
(B)
5
4
3
2
1
0
AMF(6)
HTST(6)
AMF(10)
ST(6)
OL(6)
HTOL(6)
HTAMF(6)
HTAMF(10)

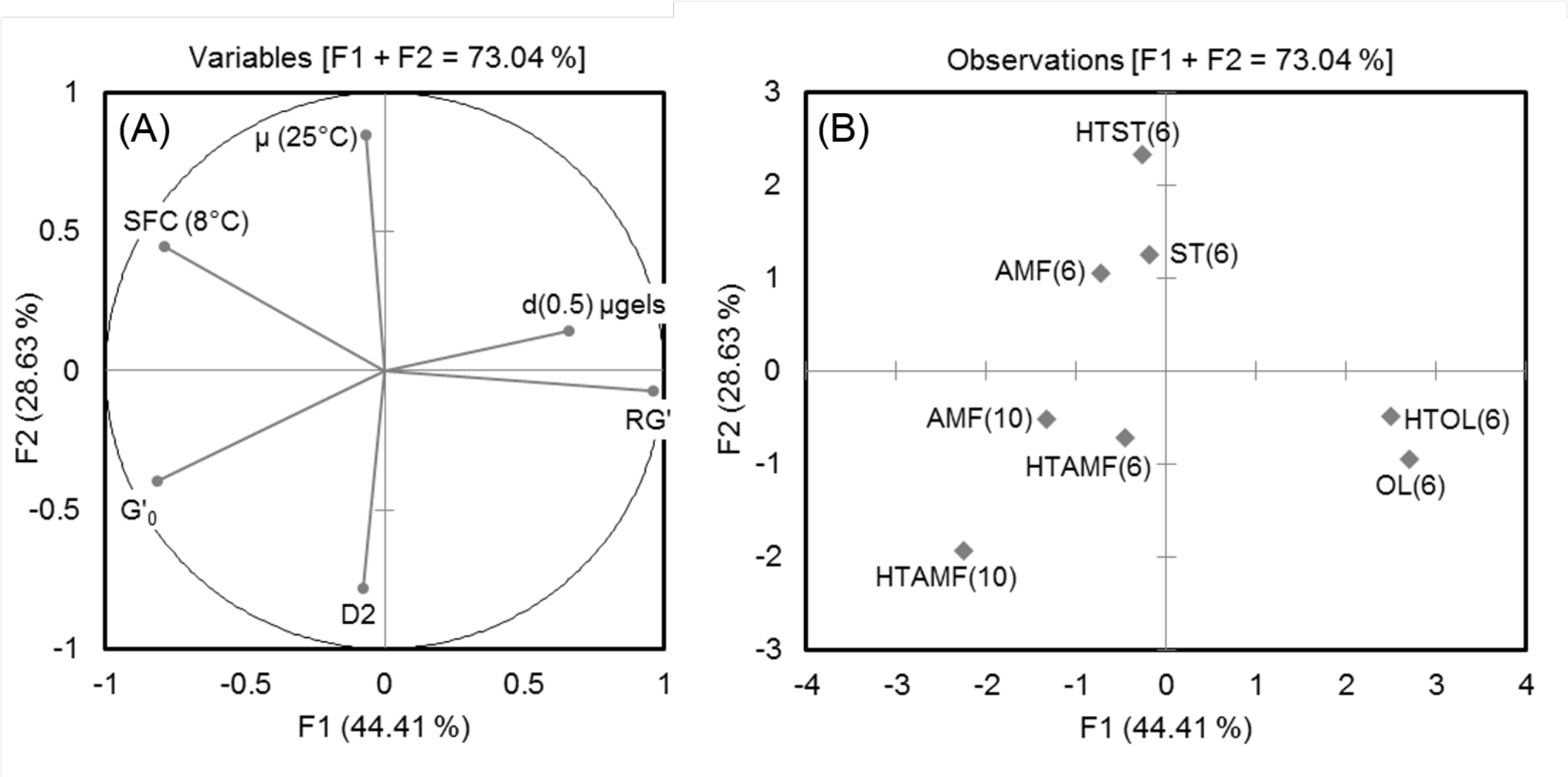
Variables [F1 + F2 = 73.04 %]
(A)
μ (25°C)
SFC (8°C)
d(0.5) μgels
RG'
G'0
D2
F2 (28.63 %)
F1 (44.41 %)
1
0.5
0
-0.5
-1
Observations [F1 + F2 = 73.04 %]
(B)
HTST(6)
ST(6)
AMF(6)
AMF(10)
HTAMF(6)
HTOL(6)
OL(6)
HTAMF(10)
F2 (28.63 %)
F1 (44.41 %)
3
2
1
0
-1
-2
-3
-4
-3
-2
-1
0
1
2
3
4

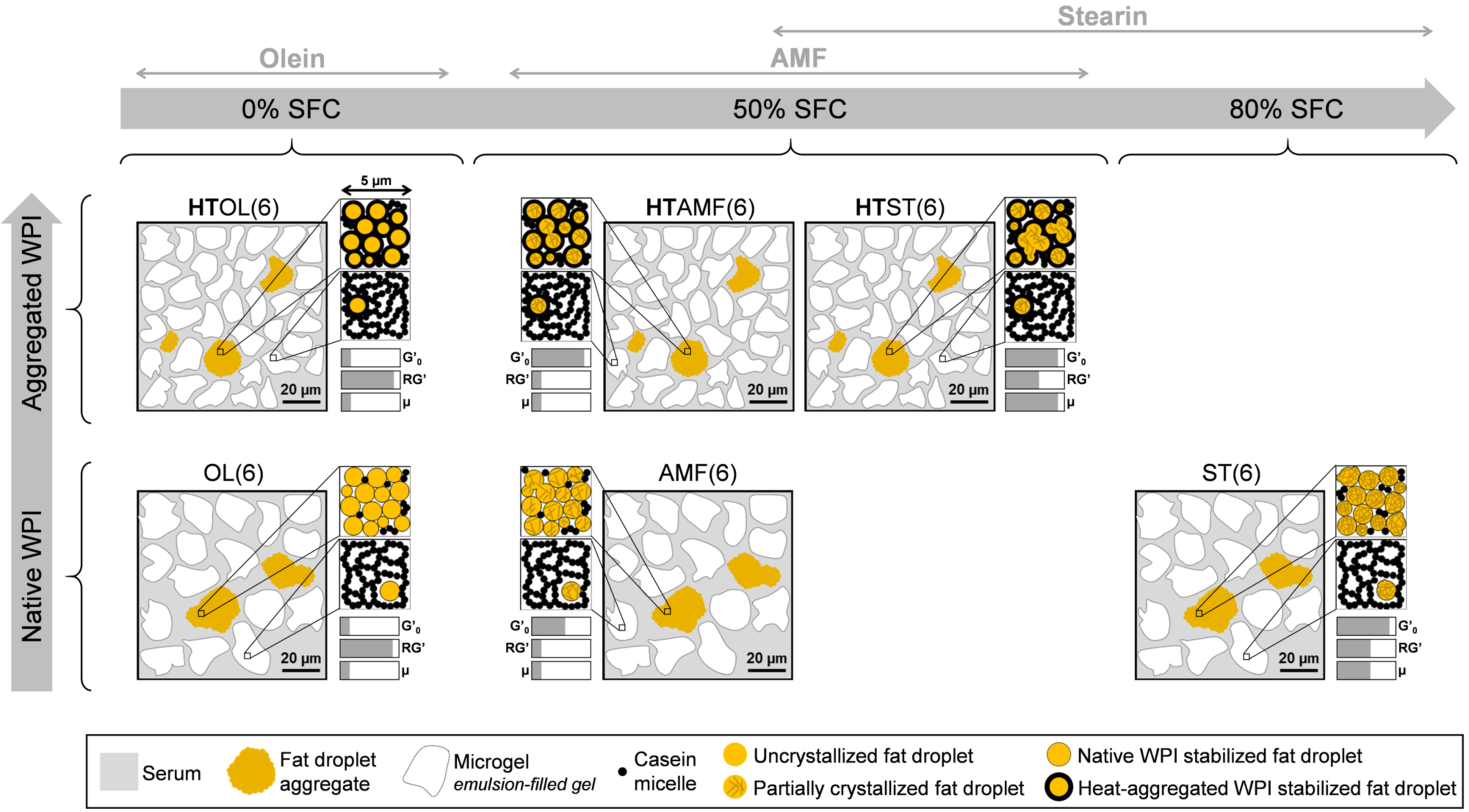
Stearin
Olein
AMF
0% SFC
50% SFC
80% SFC
Aggregated WPI
Native WPI
HTOL(6)
5 µm
20 µm
G'0
RG'
µ
HTAMF(6)
HTST(6)
OL(6)
AMF(6)
ST(6)
Serum
Fat droplet aggregate
Microgel emulsion-filled gel
Casein micelle
Uncrystallized fat droplet
Partially crystallized fat droplet
Native WPI stabilized fat droplet
Heat-aggregated WPI stabilized fat droplet

Table 1

Composition of the different types of fat used determined by GC-MS. [a]

Type of fat	AMF	Olein	Stearin
Degree of unsaturation (%)	34.3 ± 0.8	41.4 ± 4.1	25.4 ± 2.7
C18:0 (stearic acid) (%)	11.0 ± 1.4	8.2 ± 1.2	12.9 ± 2.2
C18:1 (oleic acid) (%)	30.0 ± 0.5	36.4 ± 3.9	22.4 ± 2.6
C18:2 (linoleic acid) (%)	2.3 ± 0.1	2.5 ± 0.2	1.5 ± 0.2

[a] Values are the average ± standard deviation of 3 repetitions.

Table 2

Composition, treatment and labelling of the creams and stirred milk gels. [a]

Treatment applied to aggregate the proteins in WPI solution	Types of fat	Labelling of the creams with 30 or 60 wt% fat	Fat content(s) of stirred milk gels (wt%)	Labelling of the stirred milk gels
No treatment (native)	AMF	AMF	6 or 10	AMF(6) or AMF(10)
No treatment (native)	OL	OL	6	OL(6)
No treatment (native)	ST	ST	6	ST(6)
HT at 80 °C for 30 min	AMF	HTAMF	6 or 10	HTAMF(6) or HTAMF (10)
HT at 80 °C for 30 min	OL	HTOL	6	HTOL(6)
HT at 80 °C for 30 min	ST	HTST	6	HTST(6)

[a] Abbreviations are: HT, heat-treatment; AMF, anhydrous milk fat; OL, olein fraction; ST, stearin fraction.

Table 3

Median diameters [d(0.5)] and span of the size distributions of fat droplets in the creams (30 %wt fat) (measured in Milli-Q water). [a]

Creams	d(0.5) (µm)	Span
HTAMF(10)	2.1 ± 0.0 [a]	1.5 ± 0.1 [c]
AMF(10)	1.4 ± 0.2 [c]	2.3 ± 0.4 [a]
HTAMF(6)	2.1 ± 0.0 [a]	1.5 ± 0.1 [c]
AMF(6)	1.4 ± 0.2 [c]	2.3 ± 0.4 [a]
HTST(6)	2.1 ± 0.1 [a]	1.6 ± 0.1 [b,c]
ST(6)	1.7 ± 0.0 [b]	1.6 ± 0.2 [b,c]
HTOL(6)	2.1 ± 0.1 [a]	1.5 ± 0.1 [c]
OL(6)	1.6 ± 0.1 [b,c]	1.8 ± 0.0 [b]

[a] Values with different letters in one column are significantly different at $p \leq 0.05$.

Table 4

Textural properties through (i) the storage moduli and the apparent viscosities at the beginning (G'_0, η_0) and at the end (G'_f, η_f) of rheological oral processing, and (ii) the changes they underwent (RG', Rη) between the beginning and the end of rheological oral processing. [a]

Stirred milk gels	G'_0 (Pa)	G'_f (Pa)	η_0 (Pa s)	η_f (Pa s)	RG'	Rη	μ
HTAMF(10)	190 ± 20 [a]	70 ± 15 [a]	0.99 ± 0.04 [a]	0.69 ± 0.03 [a]	0.36 ± 0.05 [c]	0.7 ± 0.03 [d]	0.21 ± 0.02 [c]
AMF(10)	160 ± 20 [b]	60 ± 5 [a]	0.82 ± 0.07 [b]	0.59 ± 0.04 [b]	0.37 ± 0.02 [c]	0.72 ± 0.01 [c,d]	0.19 ± 0.01 [c]
HTAMF(6)	90 ± 10 [c]	30 ± 2 [b,c]	0.54 ± 0.04 [c]	0.41 ± 0.03 [c,d]	0.37 ± 0.02 [c]	0.75 ± 0.02 [b,c]	0.21 ± 0.02 [c]
AMF(6)	80 ± 5 [c,d]	30 ± 5 [c]	0.47 ± 0.02 [c,d]	0.36 ± 0.01 [c,d]	0.4 ± 0.01 [b,c]	0.76 ± 0.01 [b]	0.23 ± 0.02 [b,c]
HTST(6)	90 ± 10 [c]	40 ± 5 [b,c]	0.53 ± 0.05 [c]	0.39 ± 0.03 [c,d]	0.43 ± 0.01 [b]	0.74 ± 0.02 [b,c]	0.32 ± 0.06 [a]
ST(6)	100 ± 30 [c]	40 ± 10 [b]	0.56 ± 0.14 [c]	0.43 ± 0.1 [c]	0.44 ± 0.02 [b]	0.77 ± 0.02 [b]	0.27 ± 0.02 [b]
HTOL(6)	60 ± 15 [d]	35 ± 5 [b,c]	0.4 ± 0.07 [d]	0.33 ± 0.06 [d]	0.61 ± 0.04 [a]	0.83 ± 0.01 [a]	0.23 ± 0.02 [b,c]
OL(6)	60 ± 5 [d]	30 ± 5 [b,c]	0.41 ± 0.03 [d]	0.34 ± 0.03 [d]	0.59 ± 0.02 [a]	0.83 ± 0.01 [a]	0.19 ± 0.01 [c]

[a] The friction coefficient (μ) was obtained by tribology at 25 °C; values in the same column with different superscript letters are significantly different at $p \leq 0.05$.

Table 5

Average diameters [d(0.5)] and span of the size distributions of the microgels of the stirred milk gels. [a]

Stirred milk gels	d(0.5) (µm)	Span
HTAMF(10)	11 ± 1 [d]	1.8 ± 0.3 [a]
AMF(10)	15 ± 2 [c]	1.6 ± 0.1 [b]
HTOL(6)	17 ± 3 [b,c]	1.4 ± 0.1 [b]
HTAMF(6)	16 ± 2 [c]	1.6 ± 0.1 [b]
HTST(6)	15 ± 2 [c]	1.5 ± 0.1 [b]
OL(6)	20 ± 1 [a,b]	1.5 ± 0.1 [b]
AMF(6)	20 ± 2 [a]	1.5 ± 0.1 [b]
ST(6)	21 ± 3 [a]	1.5 ± 0.2 [b]

[a] Values with different superscript letters in the same column are significantly different at $p \leq 0.05$.

Table 6

Pearson's correlation coefficients between the properties used in Fig. 6. [a]

Variables	G'_0	RG	μ (25 °C)	SFC (8 °C)	d(0.5) μgels	D2
G'_0	1	-	-	-	-	-
RG	**- 0.67**	1	-	-	-	-
μ (25 °C)	- 0.20	- 0.06	1	-	-	-
SFC (8 °C)	+ 0.46	**- 0.82**	+ 0.41	1	-	-
d(0.5) μgels	- 0.48	+ 0.59	+ 0.11	- 0.19	1	-
D2	+ 0.39	- 0.01	- 0.41	- 0.16	+ 0.07	1

[a] Values in bold indicate significant correlations between properties at $p \leq 0.1$.